

Heat increases experienced racial segregation in the United States

Till Baldenius^{1,2}, Nicolas Koch^{1,3,4,*}, Hannah Klauber¹, and Nadja Klein^{2,5}

¹Mercator Research Institute on Global Commons and Climate Change (MCC)

²Chair of Statistics and Data Science (Humboldt-Universität zu Berlin)

³Potsdam Institute for Climate Impact Research (PIK)

⁴IZA Institute of Labor Economics

⁵Chair of Uncertainty Quantification and Statistical Learning, Research Center Trustworthy Data Science and Security (UA Ruhr) and Department of Statistics (Technische Universität Dortmund)

June 2023

Abstract

Segregation on the basis of ethnic groups stands as a pervasive and persistent social challenge in many cities across the globe. Public spaces provide opportunities for diverse encounters but recent research suggests individuals adjust their time spent in such places to cope with extreme temperatures. We evaluate to what extent such adaptation affects racial segregation and thus shed light on a yet unexplored channel through which global warming might affect social welfare. We use large-scale foot traffic data for millions of places in 315 US cities between 2018 and 2020 to estimate an index of experienced isolation in daily visits between whites and other ethnic groups. We find that heat increases segregation. Results from panel regressions imply that a week with temperatures above 33°C in a city like Los Angeles induces an upward shift of visit isolation by 0.7 percentage points, which equals about 14% of the difference in the isolation index of Los Angeles to the more segregated city of Atlanta. The segregation-increasing effect is particularly strong for individuals living in lower-income areas and at places associated with leisure activities. Combining our estimates with climate model projections, we find that stringent mitigation policy can have significant co-benefits in terms of cushioning increases in racial segregation in the future.

Keywords: racial segregation, climate change, heat, foot traffic data, urban mobility

* Corresponding author: Nicolas Koch, Mercator Research Center on Global Commons and Climate Change (MCC), Torgauer Straße 12-15, 10829 Berlin, (koch@mcc-berlin.net)

1 Introduction

The negative effect of racial segregation on the socio-economic status of individuals from minority groups has been examined extensively in sociological, geographic and economic studies Massey et al. 1987, Massey 1990, Cutler and Glaeser 1997. Specifically, crime and violence (Massey 1995, Krivo et al. 2009, Light and Thomas 2019), labor market opportunities (Kain 1968), education (Sharkey and Elwert 2011), health (Collins and Williams 1999, Almond et al. 2006), and intergenerational mobility (Chetty et al. 2014, März et al. 2022, Chetty and Hendren 2018) are adversely related to racial segregation. These findings are largely limited to residency as a determinant of segregation, although daily encounters at work and leisure activities also strongly shape our experience. To better understand the dynamics of racial segregation beyond residency, segregation in the activity space, i.e. the set of all spaces in which people move in their daily lives, has become the prime object of investigation Wong and Shaw 2011, Wang et al. 2018, Athey et al. 2021. An important insight from this recent literature is that segregation is much lower when individuals spend time outside of their neighborhoods or in public spaces such as parks, restaurants and bars, or accommodation establishments Davis et al. 2019, Athey et al. 2021.

At the same time, a separate strand of literature on the impacts of climate change on human activity suggests that individuals use leisure and outdoor activity substitution as a behavioral adaptation strategy to extreme temperature (Carman and Zint 2020, Berrang-Ford et al. 2021). In particular, there is evidence that outdoor leisure activity is significantly depressed when it is hot Zivin and Neidell 2014, Obradovich and Fowler 2017, Dundas and von Haefen 2020, Fan et al. 2023. This raises the important question whether and to what extent climate adaptation behaviors may increase the extent of segregation individuals experience. If time spent in lower-segregation outdoor leisure places, such as green or blue space, is particularly affected by heat, hot weather could increase racial segregation. However, the ultimate effect depends on how individuals substitute outdoor leisure for other activities subject to varying degrees of segregation. For instance, restaurants or bars are also associated with comparatively low levels of segregation and heat-induced substitution to these public spaces could leave overall segregation unchanged. To the best of our knowledge, the heat-segregation nexus has not been addressed as the two strands of literature on climate impacts and social segregation remained detached so far.

We contribute to resolving this deficiency and shed light on the effect of heat exposure on racial segregation by coupling foot traffic data for millions

of places with spatial and temporal variations in temperature to derive the effects hot temperatures induce on segregation in the United States (US). Our large-scale foot traffic data is aggregated from app-tracking-based cell phone geolocation data collected by SafeGraph SafeGraph 2022 in 315 metropolitan statistical areas (MSAs) across the US between January 2018 and March 2020. It includes weekly counts of visits and visitors to almost eight million points of interest (POI) by the census block groups (CBGs) of visitors’ residences, for which we infer the racial composition using census data. Building on prior contributions Gentzkow and Shapiro 2011, Athey et al. 2021, we compute an index of weekly experienced isolation in visits. The index provides an estimate of how much less likely it is for a non-*White* visit to coincide with a *White* visit than it is for a *White* visit. We infer the heat exposure of visits within MSAs using daily data from the Parameter-elevation Regressions on Independent Slopes Model (PRISM) climate mapping system PRISM Climate Group 2022.

Our empirical strategy follows the well-established climate–econometric literature (Dell et al. 2014, Carleton and Hsiang 2016, Hsiang 2016) and applies fixed-effects panel regression models to exploit week-to-week variation of temperature and visit isolation within MSAs (see Model Specification). It allows us to flexibly control for time-constant differences between MSAs, weekly nationwide shocks, and state-specific trends and seasonality at the monthly level in visit isolation and temperature. We argue that temperature variation net of these fixed effects is plausibly random, allowing causal interpretation of statistically significant estimates. Compared with survey data that is often limited by self-reporting bias and a small set of respondents, our app-tracking-based data provided by SafeGraph give a more objective and representative picture of human activity under heat exposure. We show that the data are representative in terms of sex, age, education, and race, while wealthy households are slightly over-represented (see Appendix Figs. 7-11).

2 Data

Foot-traffic Data

We use data on about eight million POI, that is, geographic locations such as restaurants, grocery stores, urban transit systems, and nature parks, provided by the US company SafeGraph. The 2017 North American Industry Classification System (NAICS) codes associated with the respective establishments allow for a detailed categorization of POI.

Information on foot traffic to the POI is provided with the *Weekly Patterns* dataset, which is available as of January 1, 2018. When accessed in March 2022, *Weekly Patterns* covered an average of 0.052 devices per person in the MSAs of the CONUS. SafeGraph combines geometric information about places with location data from smartphone application users to determine visits to POI. When using an application whose provider partners with SafeGraph, geolocation pings that indicate the location of a device when used for the purposes of the application are collected via app-tracking. If such a ping is within a building’s geographic footprint and the next ping at least four minutes apart is in the same polygon, SafeGraph calls this a visit. These aggregations include the numbers of visits and visitors. For each POI, the number of visitors is broken down by the visitors’ home CBGs.

To determine the origin neighborhood of visitors, SafeGraph infers a device’s home location from its primary nighttime geohash7 (a geographical unit from a grid of approximately 500×500 feet) determined from at least six weeks of tracking. This geohash7 is then mapped to the corresponding CBG, the highest geographic resolution for which demographic data are available from the census. Linking SafeGraph data with demographic information from the census, we conclude that the data is representative of sex, age, education, and race, while wealthy households are slightly over-indexed (see Appendix Figs. 7-11).

SafeGraph data are widely used in academic research, particularly in articles related to the COVID-19 pandemic (Allcott et al. 2020, Benzell et al. 2020, Chang et al. 2021, Ma et al. 2021, Li et al. 2022, Jay et al. 2022). Specifically, these authors examine how social segregation was affected by the pandemic Park et al. 2021, Li et al. 2022, whether racial segregation differs between students and adults Cook et al. 2022, and they explore differences in movement patterns of population sub-groups Chen and Pope 2020, Prestby et al. 2020.

Weather Data and Climate Projections

The Parameter-elevation Regressions on Independent Slopes Model (PRISM) climate mapping system (PRISM Climate Group 2022), developed in the 1990s, provides official climate data of the CONUS for the Department of Agriculture of the United States. One of the PRISM products is the daily time series of CONUS weather variables, including minimum and maximum temperature as well as precipitation. The estimates are available from 1981 and are gridded at a resolution of approximately 4km. The focus of this product is to obtain the best possible estimates regardless of temporal consistency and thus uses all weather stations available at the

time of estimation (PRISM Climate Group 2022). Using the R handbook that is part of the supplementary material to ref. Ortiz-Bobea 2021, we aggregate the gridded data to the MSA level. We weight by grid-cell population (Burke et al. 2018), for which we use gridded block-level population data from ref. Falcone 2016. This method of spatial aggregation reflects the weather condition to which the average person within an MSA was exposed. We measure precipitation in millimeters and maximum temperature in degrees celsius. We consider maximum temperature because it is usually the primary measure of how hot a day is, such as in weather forecasts.

For future climate projections, we consult bias-corrected daily maximum temperatures from the Geophysical Fluid Dynamics Laboratory’s Princeton Earth System Model (GFDL-ESM4) (Lange and Büchner 2021). The model belongs to the global climate models in the sixth phase of the Coupled Model Intercomparison Project (CMIP-6). We obtain the data for the year 2050 for a best-case scenario with strict climate policy (SSP1/RCP2.6) and a worst-case scenario without emissions abatement (SSP5/RCP8.5). To aggregate the projection data to the MSA level, we apply the same procedure as to the PRISM data.

3 Methodology

Visit Isolation Index Estimation

For derivation of an index of racial segregation, we divide visitors into the groups *White* and non-*White* based on their home CBG Athey et al. 2021. Using 2010 census data, we classify a CBG as *White* if the majority of the population of that CBG identifies as White, and otherwise as non-*White*. Based on this distinction, visits originating from a particular CBG are referred to as *White* or non-*White*. Alternatively, race could be assigned to individual visits by stochastic imputation based on the racial composition of the origin CBG. However, this could lead to an underestimation of the extent of segregation because it implies that residents of the same CBG are equally likely to visit POI regardless of self-reported race (Athey et al. 2021).

While our goal is to best reflect individual experiences in the segregation measure used for our analysis, devices are not identified across locations in Weekly Patterns. This makes it impossible to determine the actual activity space of any of the individuals. Therefore, our focus is on segregation in visits rather than experienced segregation. Experienced segregation is driven by two factors. One is the set of places individuals visit. If members of two groups systematically choose different places, this contributes to

segregation. This factor may reflect a preference for places close to home or work if those places are themselves segregated, it may reflect particular preferences that differ systematically by group, such as a preference for going to the movies over going to the theater, and it may reflect a possibly unconscious preference for places where one’s group is in the majority. The second factor is the number of places an individual chooses to visit in a given time. The latter factor cannot be represented by our data. Therefore, we estimate how segregated visits are rather than focusing on individuals in our analysis. Regarding the choice of space within which we want to estimate the extent of segregation, we decide to focus on MSAs, as is common in previous contributions Cutler and Glaeser 1997, Echenique and Fryer 2007, Athey et al. 2021.

We aim to construct an estimator based on the isolation index that measures segregation of visits to POI within MSAs. To this end, we define a_l^V , b_l^V and t_l^V as the number of group a , group b and total visits to POI $l \in L_m$, respectively, where L_m is the set of POI in area m . For some of these visits, people travel from outside the area in which the POI is located. Therefore, we distinguish between visits from within an MSA and visits from outside it. Our goal is to measure segregation from the perspective of those who live within the area, but to consider that this perspective is also influenced by those who visit POIs from outside the area. With that in mind, we define *exposure* as

$$E_{a \times b, m} = \sum_{j \in A_m^V} \frac{1}{|A_m^V|} \frac{b_{l(j)}^V}{t_{l(j)}^V}, \quad (1)$$

where A_m^V denotes the set of visits of individuals from group a that have home locations in area m . Defining $b_{l,m}^V$ as the visits count to location l of individuals from group b that live in area m , we can reformulate Eq. 1 as

$$E_{a \times b, m} = \sum_{l \in L_m} \frac{a_{l,m}^V}{|A_m^V|} \frac{b_l^V}{t_l^V}. \quad (2)$$

Note that the first factor only considers visitors that reside in area m , whereas the second factor accounts for all visitors with home locations in

the United States. Substituting the *exposure* measure E into the isolation index Athey et al. 2021 yields the visit isolation index

$$VI_m = \sum_{j \in B_m^V} \frac{1}{|B_m^V|} \frac{b_{l(j)}^V}{t_{l(j)}^V} - \sum_{j \in A_m^V} \frac{1}{|A_m^V|} \frac{b_{l(j)}^V}{t_{l(j)}^V} \quad (3)$$

$$= \sum_{l \in L_m} \frac{b_{l,m}^V}{|B_m^V|} \frac{b_l^V}{t_l^V} - \sum_{l \in L_m} \frac{a_{l,m}^V}{|A_m^V|} \frac{b_l^V}{t_l^V}, \quad (4)$$

which is our preferred estimator of the extent of segregation. For this purpose, we apply the distinction of non-*White* and *White* visits defined earlier. We call these groups nw and w , respectively, and the visit isolation index becomes

$$VI_m = \sum_{l \in L_m} \frac{w_{l,m}^V}{|W_m^V|} \frac{w_l^V}{t_l^V} - \sum_{l \in L_m} \frac{nw_{l,m}^V}{|NW_m^V|} \frac{w_l^V}{t_l^V}. \quad (5)$$

It follows that, on scale of zero to unity, the visit isolation index VI_m estimates the extent to which the population that identifies as White is exposed to itself more than the population that identifies as non-White is exposed to it.

Unfortunately, we only know how many different individuals from a given home CBG stayed at a given POI at least once in a given week, but not whether they visited the POI multiple times and, if so, how many times. It follows that we can only estimate the visit isolation index of Eq. 5. To estimate visits by group based on the available information, we multiply the number of visitors at a given location, nw_i^N and w_i^N , by the visits per visitor at that location, t_l^V/t_l^N . We estimate the total number of visits by the two groups in area m in a similar manner as

$$|\widehat{NW}_m^V| := \sum_{l \in L_m} \widehat{nw}_{l,m}^V := \sum_{l \in L_m} nw_{l,m}^N \frac{t_l^V}{t_l^N}, \quad (6)$$

where is $|\widehat{NW}_m^V|$ defined accordingly. Finally, our estimator of visit isolation is

$$VI_m^{\text{est}} = \sum_{l \in L_m} \frac{\widehat{w}_{l,m}^V}{|\widehat{W}_m^V|} \frac{\widehat{w}_l^V}{t_l^V} - \sum_{l \in L_m} \frac{\widehat{nw}_{l,m}^V}{|\widehat{NW}_m^V|} \frac{\widehat{w}_l^V}{t_l^V} \quad (7)$$

Fig. 1 shows averages of weekly visit isolation estimates from January 1, 2018–March 8, 2020. We choose this period to precede potentially COVID-19-induced changes in mobility behavior to eliminate a potential source of confounding. There are 65 MSAs with insufficient non-*White* visits that

are colored gray on the map, because they have an insufficient number of recorded visits from non-*White* CBGs, which are excluded from the analysis, limiting our sample to 315 MSAs.

Model Specification

To examine the relationship between heat and the visit isolation index by exploiting temporal variation, we fit the fixed effects model

$$VI_{i\tau}^{\text{est}} = H_{i\tau}\beta + P_{i\tau}\rho + \mu_i + \delta_\tau + \eta_{sm} + \epsilon_{i\tau}, \quad (8)$$

where $i = 1, \dots, N = 315$ and $\tau = 1, \dots, T = 114$ denote MSA and week, respectively. $VI_{i\tau}^{\text{est}}$ indicates the estimator of the visit isolation index as denoted by Eq. 7 and $H_{i\tau}$ and $P_{i\tau}$ are $(1 \times k_H)$ and $(1 \times k_P)$ vectors of daily maximum temperature bins and daily precipitation bins, respectively. The associated coefficients are denoted by the vector $\beta \in \mathbb{R}^{k_H \times 1}$ and $\rho \in \mathbb{R}^{k_P \times 1}$, with β being the main coefficient of interest. There are MSA fixed effects μ_i , week fixed effects δ_τ and a third set of fixed effects η_{sm} that account for time trends specific to the states s and months m in our preferred specification. Finally, $\epsilon_{i\tau}$ denotes the error term.

The term fixed effect refers to the fact that we model μ_i and $\xi_{i\tau} := [\delta_\tau, \eta_{i\tau}]$ as parameters and thus allow for arbitrary correlation with $X_{i\tau} := [H_{i\tau}, P_{i\tau}]$.

In this case, assuming

$$E[\epsilon_{i\tau} | X_{i1}, \dots, X_{iT}, \mu_i, \xi_{i1}, \dots, \xi_{iT}] = 0, \quad \tau = 1, \dots, T, \quad (9)$$

is sufficient to obtain strict exogeneity of the form

$$E[\epsilon_{i\tau} | X_{i1}, \dots, X_{iT}] = 0, \quad \tau = 1, \dots, T. \quad (10)$$

Since they were prominently applied in a climate-agriculture Deschênes and Greenstone 2007, panel data approaches employing fixed effects have been widely used in the climate econometrics literature. In the specific case of regressions involving weather variables, deviations of weather variables from their unit-specific averages are presumed to be as good as random after controlling for temporal shocks (Deschênes and Greenstone 2007). This plausibly random weather variation net of fixed effects establishes quasi-experimental conditions, thus allowing for the identification of causal effects (Dell et al. 2014).

When employing fixed effects, time-constant characteristics of the units that may correlate with both the outcome and the variables of interest, and may thus bias the estimates, do not need to be explicitly modeled

(Wooldridge 2010, Hsiang 2016). Nevertheless, there could be time-varying factors that correlate with $X_{i\tau}$ after controlling for temporal shocks via δ_τ and $\eta_{i\tau}$. The distribution of $X_{i\tau}$ is determined by geophysical processes though and therefore other relevant climatic variables not characterized by $X_{i\tau}$ already are the main concern here (Hsiang 2016). Including additional non-climatic variables could itself be a problem, as these could themselves be affected by weather variation and therefore bias estimates by over-controlling (Dell et al. 2014). We argue that the deviation of weather variables from their MSA-specific averages after controlling for country-wide weekly and state-wide monthly shocks is as good as random and thus uncorrelated with other determinants of segregation. If this is the case and the model is correctly specified, then strict conditional exogeneity as in Eq. 10 holds in our preferred specification, making the estimator $\hat{\beta}$ unbiased and causally interpretable.

4 Results

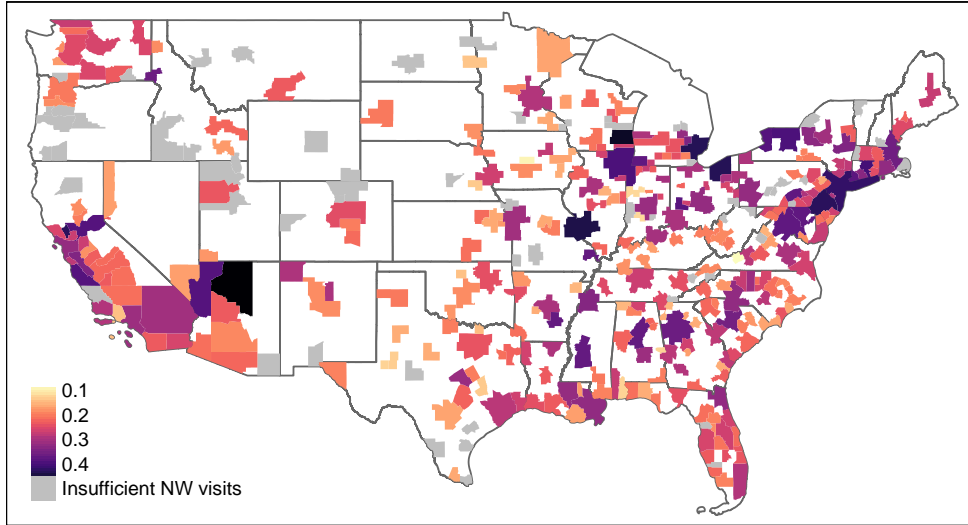
Our outcome of interest is a visit isolation index that measures racial segregation in visits to POI within MSAs (see VI Index Estimation). Fig. 1 and Fig. 2 show the average visit isolation index across 315 MSAs and how visit isolation varies over time in the three most populous MSAs, respectively. Isolation tends to be higher in the more populous MSAs compared with the smaller MSAs. The visit isolation index of about 0.4 in New York implies that a visit from a majority White CBG is 40 percentage points more likely to coincide with another visit from a majority White CBG than a visit from a majority non-White CBG.

Fig. 3a shows the estimated effect of maximum temperatures on visit isolation. We form 5°C temperature bins and count the number of days within a week on which the maximum temperature was in a given bin to model heat exposure. Thus, we model the temperature-segregation relationship flexibly. Each of the individual coefficients is interpretable as the change in estimated visit isolation associated with an additional day of maximum temperature in the respective bin relative to the reference bin of 20°C to 25°C.

Main Results

We find a U-shaped relationship between temperature and visit isolation. While the effects of additional cold days on our visit isolation index are positive but statistically insignificant, our estimates suggest a strong effect of days with high temperature on visit isolation. Fig. 3a reveals that an additional very hot day (up to 35°C and higher) is associated with a sta-

Figure 1: Average visit isolation index



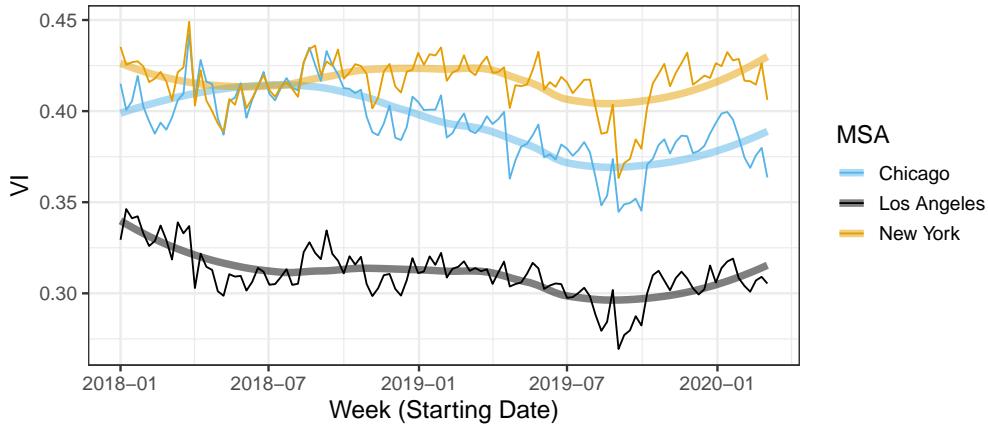
Average visit isolation index estimates for the MSAs in the CONUS, January 1, 2018–March 8, 2020. Light-colored areas indicate lower estimates of isolation. Gray-shaded areas did not have any visits labeled non-*White* in at least one time period and thus isolation could not be estimated in all time periods.

tistically significant 0.17 percentage point increase in the isolation index relative to an additional mild day (up to 20°C to 25°C). In other words, we estimate that in order for the probability of a non-*White* visit to coincide with a *White* visit to cumulatively decrease by more than one percentage point relative to the probability of a *White* visit to coincide with another *White* visit, six additional very hot days (16 days of up to 30°C to 35°C; 23 days of up to 25°C to 30°C) are required. In order to help building some intuition about the magnitude of this effect, we provide a few benchmarks. In August 2018, Los Angeles experienced a week of average maximum temperatures above 33°C. Our estimates imply that the heat effect of such a week entails an upward shift of visit isolation by 0.7 percentage points. This shift equals about 14% of the difference in visit isolation of Los Angeles to Atlanta, 32% of the difference to Miami, and 80% to San Francisco. As an alternative benchmark, we compare our results to segregation trends. In Los Angeles, our visit isolation index shows a decreasing trend over the sample period (Fig. 2). The positive effect we find for the heat week in the city is approximately thirty times the decrease in the trend.

Robustness Checks

To control for spatial and temporal confounders of visit isolation, the inclusion of MSA and week-specific fixed effects represents a minimum require-

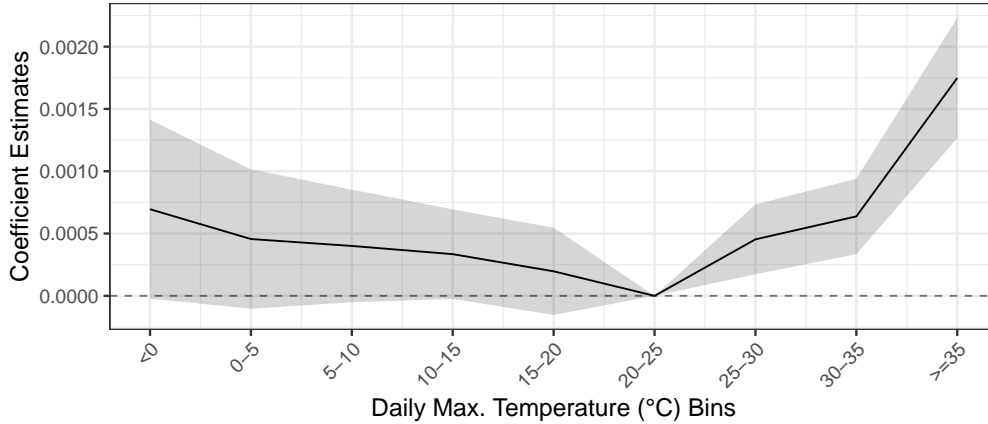
Figure 2: Visit isolation index (VI) for the three most populous MSAs



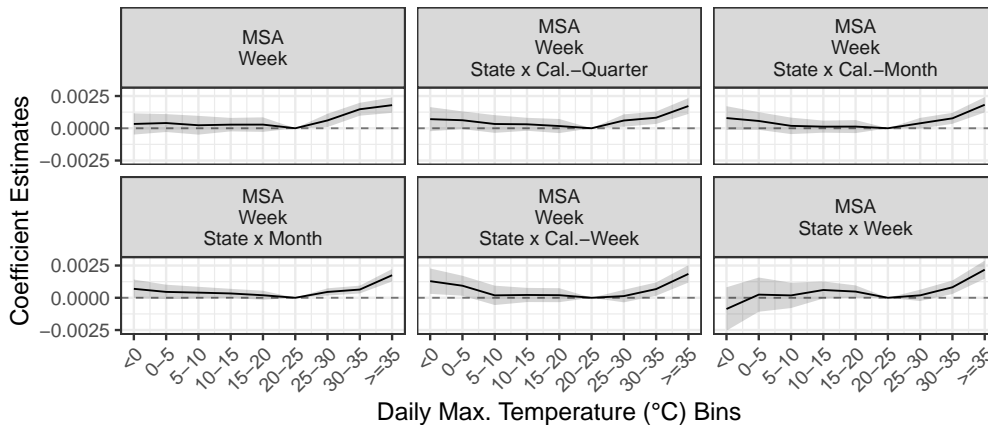
Visit isolation index (VI) estimates from January 1, 2018 – March 8, 2020 for the three most populous MSAs in the United States. The blue, black, and yellow lines refer to the MSAs of Chicago, Los Angeles, and New York, respectively. The smooth lines depict a local quadratic polynomial regression fit with span parameter $\alpha = 0.6$.

ment for our model specification. These fixed effects restrict the model to exploit only variation within MSAs and allow for flexibly absorbing nationwide time trends in the isolation index as well as effects linked to specific occasions such as national holidays, elections or big sports events. To account for potential regional time-varying sources of confounding that could be correlated with both weather and the isolation index, we include additional fixed effects at the state-month level. While we believe this fixed effects choice to be most suitable to recover the parameter of interest, the degree of stringency may be chosen differently. For this reason, Fig. 3b shows our preferred fixed effects specification in the bottom left panel along with five alternative fixed effects specifications, all of which include at minimum an MSA and a week-specific fixed effect. The panels from left to right and top to bottom are ordered by increasing level of stringency in the fixed effects. In all specifications, coefficient estimates and standard errors for high temperature bins are very robust compared to the preferred specification. Most specifications also indicate a positive but weaker effect of cold temperatures; however, it is mostly statistically insignificant. Results are also robust to computing clustered standard errors instead of Conley-HAC standard errors (see Appendix Fig. 12) and to changing the geographic area of reference from MSAs to urban areas as delineated for the US census (see Appendix Fig. 13).

Figure 3: The relationship between visit isolation and daily maximum temperature



(a) Coefficients estimated by regressing visit isolation on daily maximum temperature bins using a fixed effects model. The 20°C to 25°C bin serves as a reference bin and precipitation is included as a control variable. MSA, week, and state-by-month fixed-effects are employed and observations are weighted by MSA population size. Shaded areas depict asymptotic 95% confidence intervals based on Conley-HAC standard errors.



(b) Re-estimations of the relationship between visit isolation and daily maximum temperature with alternative fixed effects specifications as indicated by the subheadings of each panel. The preferred specification from Fig. 3a (bottom left) is compared to specifications neglecting subregional time trends (top left panel), controlling for statewide seasonality in calendar quarters (top middle), calendar months (top right), and calendar weeks (bottom middle), and statewide weekly time trends (bottom right).

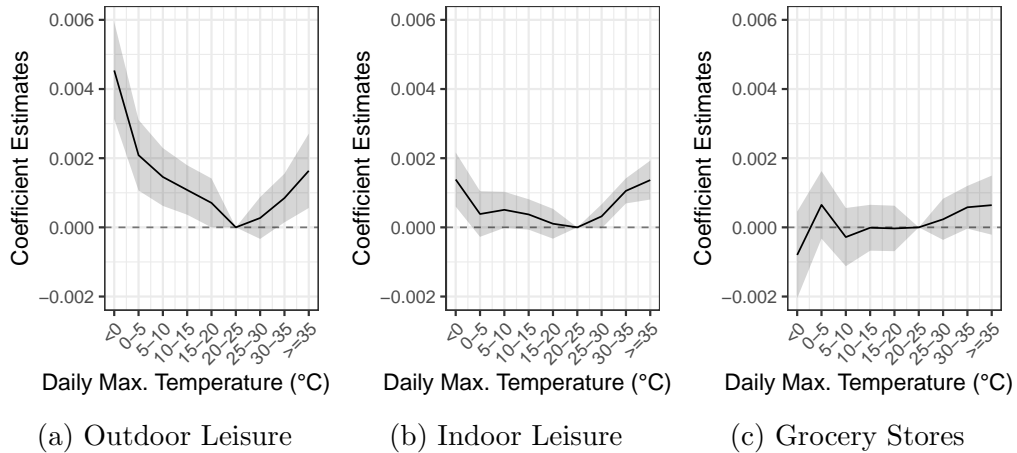
Heterogeneity Analysis

To gain an initial understanding of potential mechanisms driving the heat-isolation relationship, we analyze how the effect of heat on visit isolation is heterogeneous across three categories of places: outdoor POI associated with leisure activities, indoor POI associated with leisure activities,

and grocery stores (Figs. 4a–4c). At outdoor places, both very low and very high temperatures are associated with higher isolation compared to moderate temperatures, with the effect of cold weather being particularly strong. Indoor places show a similar relationship between high temperatures and visit isolation, while low temperatures do not have nearly as significant an effect. While decreases in leisure and outdoor activity related to hot weather have been shown in previous studies Zivin and Neidell 2014, Obradovich and Fowler 2017, Dundas and von Haefen 2020, Fan et al. 2023, we provide new evidence documenting that this adaptation to heat induces a higher degree of visit isolation. In contrast, grocery stores exhibit fairly constant levels of isolation across the weather distribution, potentially due to a lower elasticity in demand for groceries.

We also examine whether the relationship between temperature and isolation varies with MSA population size. In general, segregation patterns can vary substantially across cities. While larger cities tend to have a more diverse population overall, they may be more segregated across neighborhoods. These baseline differences may also affect how strong the potential for temperature-induced changes in segregation patterns is. For instance, moving between areas with different racial and ethnic compositions during periods of heat could constitute a greater effort in larger cities. We find that the effect of heat is strongest in MSAs of the second population size quartile, corresponding to between 300 thousand and 700 thousand

Figure 4: The relationship between visit isolation and daily maximum temperature across different places of daily activity

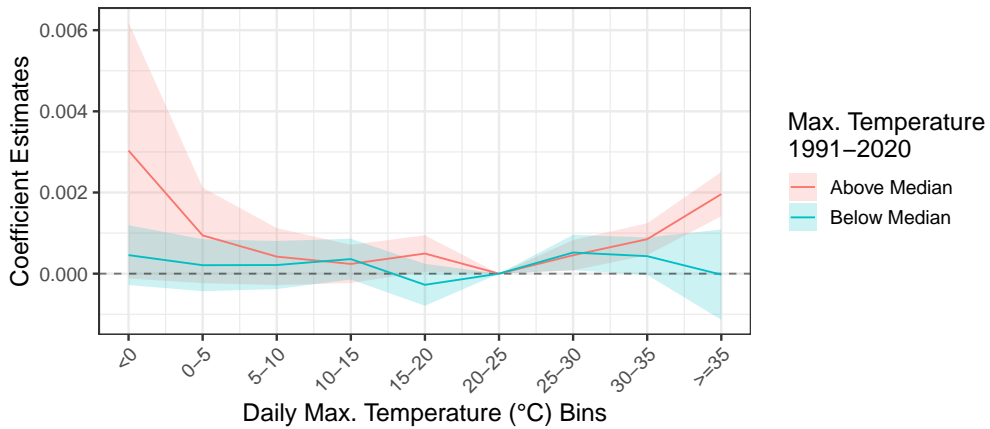


The three panels present the relationship between visit isolation and daily maximum temperature estimated at outdoor POI associated with leisure activities (4a), indoor POI associated with leisure activities (4b), and grocery stores (4c). All estimates are based on the regression specification presented in Fig. 3a.

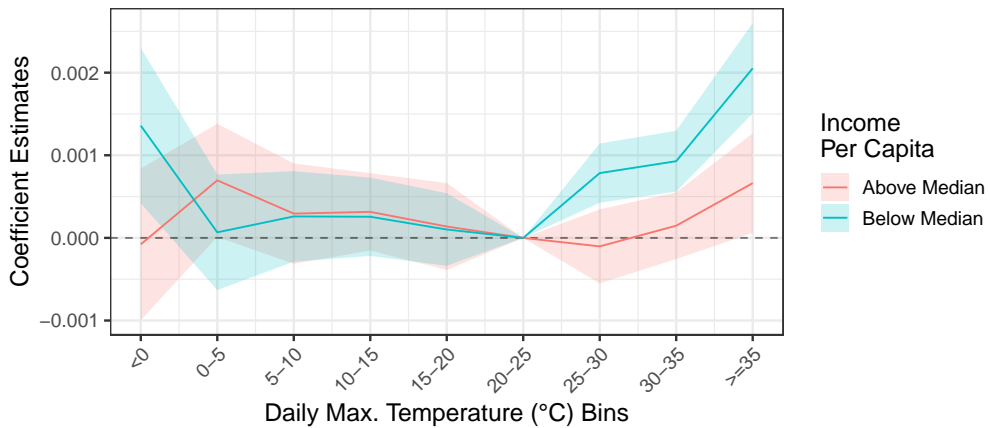
inhabitants (see Appendix Fig. 14). However, uncertainty in the estimates prevents us from identifying clear patterns of effect heterogeneity.

As a final heterogeneity analysis, we interact maximum temperature with an indicator of being above the population-weighted median of MSA-level 30-year average maximum temperature in a varying-coefficient model. Fig. 5a shows that there is a statistically differential effect only for the association between isolation and heat of at least 35°C. On such extremely hot days only MSAs in hotter climates exhibit increased isolation. This suggests that there is limited to no adaptation to hot temperatures in terms of

Figure 5: Heterogeneity in the relationship between visit isolation and daily maximum temperature



(a) MSAs below and above median 30-year normal maximum temperature



(b) MSA below and above median household income per capita

The panels present the relationship between visit isolation and daily maximum temperature when interacting weather variables with an indicator of being above the population-weighted median of 30-year normal maximum temperature (5a) and household income per capita (5b). All estimates are based on the regression specification presented in Fig. 3a.

maintaining diversity of potential encounters in cities where heat is more common. Fig. 5b shows the coefficient estimates when interacting the maximum temperature bins with an indicator for a per capita income that is above or below the population-weighted median. The estimates reveal a strong heat effect on visit isolation in poorer MSAs, whereas it is statistically insignificant in richer ones.

Heat-induced segregation in a changing climate

With progressing climate change, exposure to higher temperatures will increase. We aim to assess the potential net effect of such climatic changes on isolation. To this end, we conduct a simple *ceteris paribus* projection of the change in the number of encounters a non-*White* person today would have with a *White* person if she lived in a future climate. We proceed as follows: First, we calculate the weekly difference in the number of days per temperature bin between the two climate scenarios in 2050 and the reference period from 1987 to 2017. Second, we multiply the temperature differences with the estimated coefficients $\hat{\beta}$ from Eq. 8 and the total volume of visits. To derive the individual-level change in the number of encounters, we divide the quantities by the number of registered devices (see Fig. 6).¹

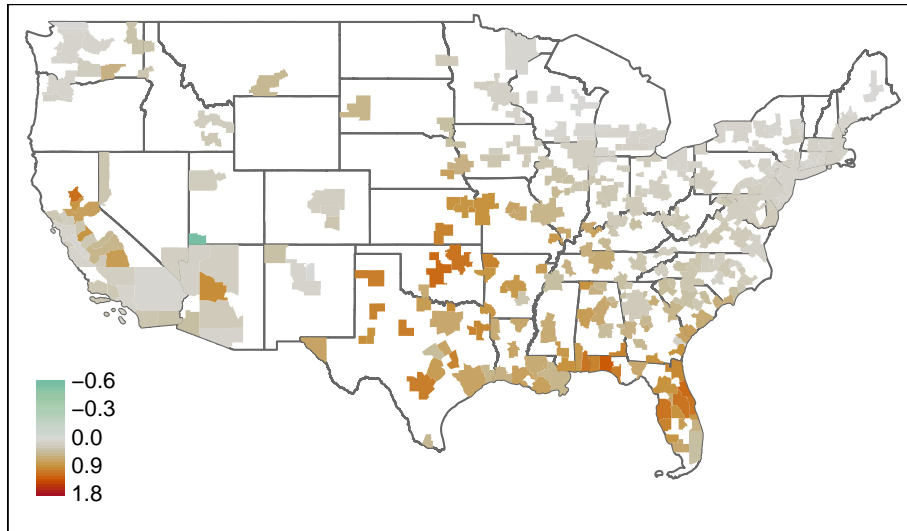
Importantly, this back-of-the-envelope projection neglects potential changes in the population composition and adaptation. Thus, it only serves as a first-order approximation of potential racial isolation under future climate change. We combine the temperature-isolation relationship estimated in Fig. 3a with two possible climate scenarios from the Sixth Assessment Report of the Intergovernmental Panel on Climate Change (IPCC). A best-case scenario represents the implementation of strict climate policy that ensures a global temperature increase well below 2°C by 2100 (SSP1/RCP2.6), and a worst-case scenario represents the absence of any emission reductions leading to a temperature rise of 4.7 to 5.1°C (SSP5/RCP8.5). We consider the change in between-group encounters in both scenarios compared to the reference period 1987-2017.

Fig. 6 shows that the encounters decrease in many MSAs in both scenarios in 2050. However, the number of MSAs that experience increasing isolation and the magnitude of the projected changes is larger in the worst-case scenario. Only one MSA in Utah exhibits a notable decrease in isolation. However, this effect decreases in magnitude from scenario SSP1/RCP2.6 to SSP5/RCP8.5, suggesting that the former scenario leads to less isolation than the latter for all MSAs despite substantial geographic heterogeneity.

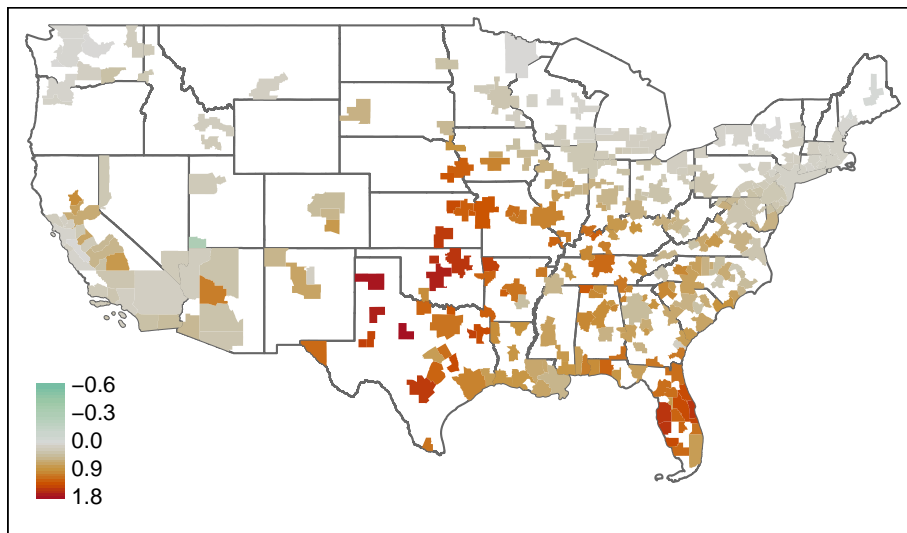
¹To obtain the population-wide change in the number of encounters per MSA, we alternatively multiply the calculated quantities with the ratio of MSA population size over the number of devices recorded by Safegraph (see Appendix Table 1).

This suggests that strong climate policy has the co-benefit of reducing temperature-induced racial isolation under global warming. In Appendix Table 1, we also approximate the total number of foregone encounters that

Figure 6: Projected change in experienced segregation under different climate scenarios



(a) Under SSP3



(b) Under SSP5

Projected change in the number of per capita encounters of non-White and White individuals in 2050 compared to the reference period from 1987 to 2017. Panel 6a refers to a best-case climate change scenario with a temperature rise of well below 2°C by 2100, Panel 6b to a worst-case scenario with a temperature rise of 4.7 to 5.1°C.

could accrue in the most affected MSAs due to a changing climate in 2050. In Dallas, for instance, global warming could eliminate up to about eight million between-group encounters compared to the annual average number of encounters in the reference period.

5 Conclusion

We find that exposure to daily maximum temperature above 25°C has a robust positive effect on an index of isolation that estimates the extent of segregation based on the probability of inter-racial encounters. Therefore, we conclude that heat positively affects racial segregation. The effect is particularly strong at places for leisure activities and for individuals living in lower-income areas. Across the temperature distribution, we find a U-shaped relationship, though effects of low temperature are mostly smaller in magnitude and less robust. We project that the net effect of climate change until the middle of the century is segregation-increasing in most MSAs. Compared to unabated warming, strict climate policy will consistently lead to less isolation across the US.

The existence of heat-induced segregation in daily life is hard to grasp quantitatively and our study provides the first evidence attesting their existence based on large-scale foot traffic data. Although the estimated effects remain moderate in absolute terms, they may indicate broader behavioral adjustments to temperatures that affect the interracial exchange and are undocumented thus far. With these insights, our study calls for further research. While we shed light on another channel through which global warming might affect social welfare, only future research can clarify just *how* this effect materializes.

Further research is needed that provides explanations for racial differences in visiting outdoor and indoor leisure places during heat periods. Our analysis hints at income-related effect differences, and other studies confirm that poverty status is an important factor in explaining segregation (Wang et al. 2018). However, only a further analysis can elucidate the specific drivers of heat-caused isolation which may include racial differences in access to different modes of transportation or the distance of residency to the POI, for instance. In addition, future research could investigate potential segregation dynamics within the two groups of *White* and non-*White* individuals that we observe. We hypothesize that there are significant differences in the average socialization, living conditions, and domains of activity of African Americans, Hispanics, Asian Americans, Native Americans, and other groups that we ignore in our simplified two-group consideration.

References

- Allcott, H., L. Boxell, J. Conway, M. Gentzkow, M. Thaler, and D. Yang (2020). Polarization and public health: Partisan differences in social distancing during the coronavirus pandemic. *Journal of Public Economics* 191, p. 104254. ISSN: 0047-2727. DOI: <https://doi.org/10.1016/j.jpubeco.2020.104254>. URL: <https://www.sciencedirect.com/science/article/pii/S0047272720301183>.
- Almond, D., K. Chay, and M. Greenstone (2006). Civil Rights, the War on Poverty, and Black-White Convergence in Infant Mortality in the Rural South and Mississippi. *MIT Department of Economics Working Paper* 07(04). DOI: [10.2139/ssrn.961021](https://doi.org/10.2139/ssrn.961021).
- Athey, S., B. Ferguson, M. Gentzkow, and T. Schmidt (2021). Estimating experienced racial segregation in US cities using large-scale GPS data. *Proceedings of the National Academy of Sciences* 118(46), e2026160118. DOI: [10.1073/pnas.2026160118](https://doi.org/10.1073/pnas.2026160118). eprint: <https://www.pnas.org/doi/pdf/10.1073/pnas.2026160118>. URL: <https://www.pnas.org/doi/abs/10.1073/pnas.2026160118>.
- Benzell, S. G., A. Collis, and C. Nicolaides (2020). Rationing social contact during the COVID-19 pandemic: Transmission risk and social benefits of US locations. *Proceedings of the National Academy of Sciences* 117(26), pp. 14642–14644. DOI: [10.1073/pnas.2008025117](https://doi.org/10.1073/pnas.2008025117). eprint: <https://www.pnas.org/doi/pdf/10.1073/pnas.2008025117>. URL: <https://www.pnas.org/doi/abs/10.1073/pnas.2008025117>.
- Berrang-Ford, L. et al. (2021). A systematic global stocktake of evidence on human adaptation to climate change. *Nature Climate Change* 11(11), pp. 989–1000. ISSN: 1758-6798. DOI: [10.1038/s41558-021-01170-y](https://doi.org/10.1038/s41558-021-01170-y). URL: <https://doi.org/10.1038/s41558-021-01170-y>.
- Burke, M., F. González, P. Baylis, S. Heft-Neal, C. Baysan, S. Basu, and S. Hsiang (2018). Higher Temperatures Increase Suicide Rates in the United States and Mexico. *Nature Climate Change* 8, pp. 723–729.
- Carleton, T. A. and S. M. Hsiang (2016). Social and economic impacts of climate. *Science* 353(6304), aad9837. DOI: [10.1126/science.aad9837](https://doi.org/10.1126/science.aad9837). eprint: <https://www.science.org/doi/pdf/10.1126/science.aad9837>. URL: <https://www.science.org/doi/abs/10.1126/science.aad9837>.
- Carman, J. P. and M. T. Zint (2020). Defining and classifying personal and household climate change adaptation behaviors. *Global Environmental Change* 61, p. 102062. ISSN: 0959-3780. DOI: <https://doi.org/10.1016/j.gloenvcha.2020.102062>. URL: <https://www.sciencedirect.com/science/article/pii/S0959378019306673>.
- Chang, S., E. Pierson, P. W. Koh, J. Gerardin, B. Redbird, D. Grusky, and J. Leskovec (2021). Mobility network models of COVID-19 explain inequities

- and inform reopening. *Nature* 589(7840), pp. 82–87. ISSN: 1476-4687. DOI: 10.1038/s41586-020-2923-3. URL: <https://doi.org/10.1038/s41586-020-2923-3>.
- Chen, M. K. and D. G. Pope (2020). Geographic Mobility in America: Evidence from Cell Phone Data. Working Paper 27072. National Bureau of Economic Research. DOI: 10.3386/w27072. URL: <http://www.nber.org/papers/w27072>.
- Chetty, R. and N. Hendren (2018). The Impacts of Neighborhoods on Intergenerational Mobility I: Childhood Exposure Effects. *The Quarterly Journal of Economics* 133(3), pp. 1107–1162. ISSN: 0033-5533. DOI: 10.1093/qje/qjy007. eprint: <https://academic.oup.com/qje/article-pdf/133/3/1107/25705047/qjy007.pdf>. URL: <https://doi.org/10.1093/qje/qjy007>.
- Chetty, R., N. Hendren, P. Kline, E. Saez, and N. Turner (2014). Is the United States Still a Land of Opportunity? Recent Trends in Intergenerational Mobility. *American Economic Review* 104(5), pp. 141–47. DOI: 10.1257/aer.104.5.141. URL: <https://www.aeaweb.org/articles?id=10.1257/aer.104.5.141>.
- Collins, C. A. and D. R. Williams (1999). Segregation and Mortality: The Deadly Effects of Racism? *Sociological Forum* 14(3), pp. 495–523. ISSN: 08848971, 15737861. URL: <http://www.jstor.org/stable/684876> (visited on 10/25/2022).
- Cook, C., L. Currier, and E. L. Glaeser (2022). Urban Mobility and the Experienced Isolation of Students and Adults. Working Paper 29645. National Bureau of Economic Research. DOI: 10.3386/w29645. URL: <http://www.nber.org/papers/w29645>.
- Cutler, D. M. and E. L. Glaeser (1997). Are Ghettos Good or Bad? *The Quarterly Journal of Economics* 112(3), pp. 827–872. ISSN: 0033-5533. DOI: 10.1162/003355397555361. eprint: <https://academic.oup.com/qje/article-pdf/112/3/827/5431883/112-3-827.pdf>. URL: <https://doi.org/10.1162/003355397555361>.
- Davis, D. R., J. I. Dingel, J. Monras, and E. Morales (2019). How Segregated Is Urban Consumption? *Journal of Political Economy* 127(4), pp. 1684–1738. DOI: 10.1086/701680. eprint: <https://doi.org/10.1086/701680>. URL: <https://doi.org/10.1086/701680>.
- Dell, M., B. F. Jones, and B. A. Olken (2014). What Do We Learn from the Weather? The New Climate-Economy Literature. *Journal of Economic Literature* 52(3), pp. 740–98. DOI: 10.1257/jel.52.3.740. URL: <https://www.aeaweb.org/articles?id=10.1257/jel.52.3.740>.
- Deschênes, O. and M. Greenstone (2007). The Economic Impacts of Climate Change: Evidence from Agricultural Output and Random Fluctuations in Weather. *American Economic Review* 97(1), pp. 354–385. DOI: 10.1257/

- aer.97.1.354. URL: <https://www.aeaweb.org/articles?id=10.1257/aer.97.1.354>.
- Dundas, S. J. and R. H. von Haefen (2020). The Effects of Weather on Recreational Fishing Demand and Adaptation: Implications for a Changing Climate. *Journal of the Association of Environmental and Resource Economists* 7(2), pp. 209–242. DOI: 10.1086/706343. eprint: <https://doi.org/10.1086/706343>. URL: <https://doi.org/10.1086/706343>.
- Echenique, F. and J. Fryer Roland G. (2007). A Measure of Segregation Based on Social Interactions. *The Quarterly Journal of Economics* 122(2), pp. 441–485. ISSN: 0033-5533. DOI: 10.1162/qjec.122.2.441. eprint: <https://academic.oup.com/qje/article-pdf/122/2/441/5470068/122-2-441.pdf>. URL: <https://doi.org/10.1162/qjec.122.2.441>.
- Falcone, J. A. (2016). *U.S. block-level population density rasters for 1990, 2000, and 2010: U.S. Geological Survey data release*. <http://dx.doi.org/10.5066/F74J0C6M>. Accessed December 4, 2022.
- Fan, Y., J. Wang, N. Obradovich, and S. Zheng (2023). Intraday adaptation to extreme temperatures in outdoor activity. *Scientific Reports* 13(1), p. 473. ISSN: 2045-2322. DOI: 10.1038/s41598-022-26928-y. URL: <https://doi.org/10.1038/s41598-022-26928-y>.
- Gentzkow, M. and J. M. Shapiro (2011). Ideological Segregation Online and Offline. *The Quarterly Journal of Economics* 126(4), pp. 1799–1839. ISSN: 0033-5533. DOI: 10.1093/qje/qjr044. eprint: <https://academic.oup.com/qje/article-pdf/126/4/1799/17089890/qjr044.pdf>. URL: <https://doi.org/10.1093/qje/qjr044>.
- Hsiang, S. (2016). Climate Econometrics. *Annual Review of Resource Economics* 8(1), pp. 43–75. DOI: 10.1146/annurev-resource-100815-095343. eprint: <https://doi.org/10.1146/annurev-resource-100815-095343>. URL: <https://doi.org/10.1146/annurev-resource-100815-095343>.
- Jay, J., F. Heykoop, L. Hwang, A. Courtepatte, J. de Jong, and M. Kondo (2022). Use of smartphone mobility data to analyze city park visits during the COVID-19 pandemic. *Landscape and Urban Planning* 228, p. 104554. ISSN: 0169-2046. DOI: <https://doi.org/10.1016/j.landurbplan.2022.104554>. URL: <https://www.sciencedirect.com/science/article/pii/S0169204622002031>.
- Kain, J. F. (1968). Housing Segregation, Negro Employment, and Metropolitan Decentralization. *The Quarterly Journal of Economics* 82(2), pp. 175–197. ISSN: 0033-5533. DOI: 10.2307/1885893. eprint: <https://academic.oup.com/qje/article-pdf/82/2/175/5350689/82-2-175.pdf>. URL: <https://doi.org/10.2307/1885893>.
- Krivo, L., R. Peterson, and D. Kuhl (2009). Segregation, Racial Structure, and Neighborhood Violent Crime. *American Journal of Sociology* 114(6), pp. 1765–

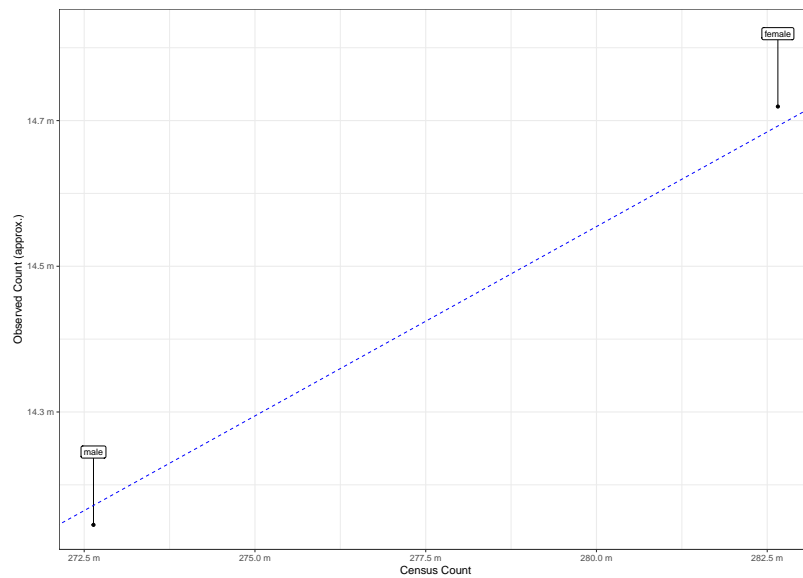
1802. DOI: [10.1086/597285](https://doi.org/10.1086/597285). eprint: <https://doi.org/10.1086/597285>. URL: <https://doi.org/10.1086/597285>.
- Lange, S. and M. Büchner (2021). ISIMIP3b Bias-adjusted Atmospheric Climate Input data (v1.1). *ISIMIP Repository*. DOI: <https://doi.org/10.48364/ISIMIP.842396.1>.
- Li, X., X. Huang, D. Li, and Y. Xu (2022). Aggravated social segregation during the COVID-19 pandemic: Evidence from crowdsourced mobility data in twelve most populated U.S. metropolitan areas. *Sustainable Cities and Society* 81, p. 103869. ISSN: 2210-6707. DOI: <https://doi.org/10.1016/j.scs.2022.103869>. URL: <https://www.sciencedirect.com/science/article/pii/S2210670722001962>.
- Light, M. T. and J. T. Thomas (2019). Segregation and Violence Reconsidered: Do Whites Benefit from Residential Segregation? *American Sociological Review* 84(4), pp. 690–725. DOI: [10.1177/0003122419858731](https://doi.org/10.1177/0003122419858731). eprint: <https://doi.org/10.1177/0003122419858731>. URL: <https://doi.org/10.1177/0003122419858731>.
- Ma, Y., S. Pei, J. Shaman, R. Dubrow, and K. Chen (2021). Role of meteorological factors in the transmission of SARS-CoV-2 in the United States. *Nature Communications* 12(1), p. 3602. ISSN: 2041-1723. DOI: [10.1038/s41467-021-23866-7](https://doi.org/10.1038/s41467-021-23866-7). URL: <https://doi.org/10.1038/s41467-021-23866-7>.
- Massey, D. S. (1990). American Apartheid: Segregation and the Making of the Underclass. *American Journal of Sociology* 96(2), pp. 329–357. DOI: [10.1086/229532](https://doi.org/10.1086/229532). eprint: <https://doi.org/10.1086/229532>. URL: <https://doi.org/10.1086/229532>.
- (1995). Getting Away with Murder: Segregation and Violent Crime in Urban America. *University of Pennsylvania Law Review* 143(5), pp. 1203–1232. ISSN: 00419907. URL: <http://www.jstor.org/stable/3312474> (visited on 10/25/2022).
- Massey, D. S., G. A. Condran, and N. A. Denton (1987). The Effect of Residential Segregation on Black Social and Economic Well-Being. *Social Forces* 66(1), pp. 29–56. ISSN: 0037-7732. DOI: [10.1093/sf/66.1.29](https://doi.org/10.1093/sf/66.1.29). eprint: <https://academic.oup.com/sf/article-pdf/66/1/29/6515004/66-1-29.pdf>. URL: <https://doi.org/10.1093/sf/66.1.29>.
- März, A., N. Klein, T. Kneib, and O. Mußhoff (2022). Intergenerational Social Mobility in the United States: A Multivariate Analysis Using Bayesian Distributional Regression. *Working paper. Available on request*.
- Obradovich, N. and J. H. Fowler (2017). Climate change may alter human physical activity patterns. *Nature Human Behaviour* 1(5), p. 0097. ISSN: 2397-3374. DOI: [10.1038/s41562-017-0097](https://doi.org/10.1038/s41562-017-0097). URL: <https://doi.org/10.1038/s41562-017-0097>.

- Ortiz-Bobea, A. (2021). Chapter 76 - The empirical analysis of climate change impacts and adaptation in agriculture. In: *Handbook of Agricultural Economics*. Ed. by C. B. Barrett and D. R. Just. Vol. 5. Handbook of Agricultural Economics. Elsevier, pp. 3981–4073. DOI: <https://doi.org/10.1016/bs.hesagr.2021.10.002>. URL: <https://www.sciencedirect.com/science/article/pii/S1574007221000025>.
- Park, J., N. M. C. Pankratz, and A. Behrer (2021). Temperature, Workplace Safety, and Labor Market Inequality. *IZA DP* No. 14560.
- Prestby, T., J. App, Y. Kang, and S. Gao (2020). Understanding neighborhood isolation through spatial interaction network analysis using location big data. *Environment and Planning A: Economy and Space* 52(6), pp. 1027–1031. DOI: 10.1177/0308518X19891911. eprint: <https://doi.org/10.1177/0308518X19891911>. URL: <https://doi.org/10.1177/0308518X19891911>.
- PRISM Climate Group (2022). *PRISM Climate Group, Oregon State University*. <http://prism.oregonstate.edu>. Accessed December 4, 2022.
- SafeGraph (2022). *SafeGraph Docs*. <https://docs.safegraph.com/docs>. Accessed Oct 21, 2022.
- Sharkey, P. and F. Elwert (2011). The Legacy of Disadvantage: Multigenerational Neighborhood Effects on Cognitive Ability. *American Journal of Sociology* 116(6), pp. 1934–1981. DOI: 10.1086/660009. eprint: <https://doi.org/10.1086/660009>. URL: <https://doi.org/10.1086/660009>.
- Wang, Q., N. E. Phillips, M. L. Small, and R. J. Sampson (2018). Urban mobility and neighborhood isolation in America’s 50 largest cities. *Proceedings of the National Academy of Sciences* 115(30), pp. 7735–7740. DOI: 10.1073/pnas.1802537115. eprint: <https://www.pnas.org/doi/pdf/10.1073/pnas.1802537115>. URL: <https://www.pnas.org/doi/abs/10.1073/pnas.1802537115>.
- Wong, D. W. S. and S.-L. Shaw (2011). Measuring segregation: an activity space approach. *Journal of Geographical Systems* 13(2), pp. 127–145. ISSN: 1435-5949. DOI: 10.1007/s10109-010-0112-x. URL: <https://doi.org/10.1007/s10109-010-0112-x>.
- Wooldridge, J. M. (2010). *Econometric Analysis of Cross Section and Panel Data, 2nd ed.* The MIT Press. ISBN: 9780262232586. URL: <http://www.jstor.org/stable/j.ctt5hhcfr> (visited on 10/18/2022).
- Zivin, J. G. and M. Neidell (2014). Temperature and the Allocation of Time: Implications for Climate Change. *Journal of Labor Economics* 32(1), pp. 1–26. ISSN: 0734306X, 15375307. URL: <http://www.jstor.org/stable/10.1086/671766> (visited on 12/04/2022).

Appendix

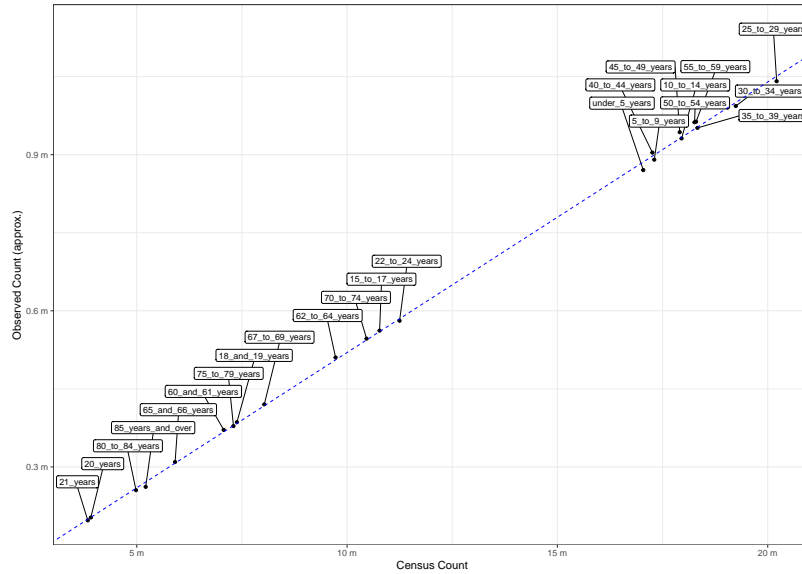
Appendix Figures

Figure 7: Representativeness of SafeGraph data in terms of sex



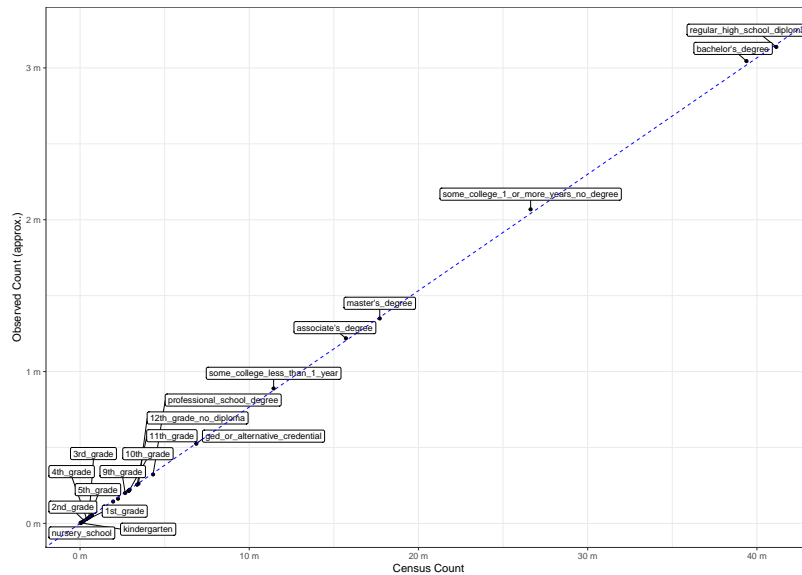
The plot shows how the sex distribution of the SafeGraph users (y-axis) relates to the sex distribution recorded by the census (x-axis). Both axes count the number of individuals in million (m). For representativeness the counts should line up along the diagonal line in blue.

Figure 8: Representativeness of SafeGraph data in terms of age



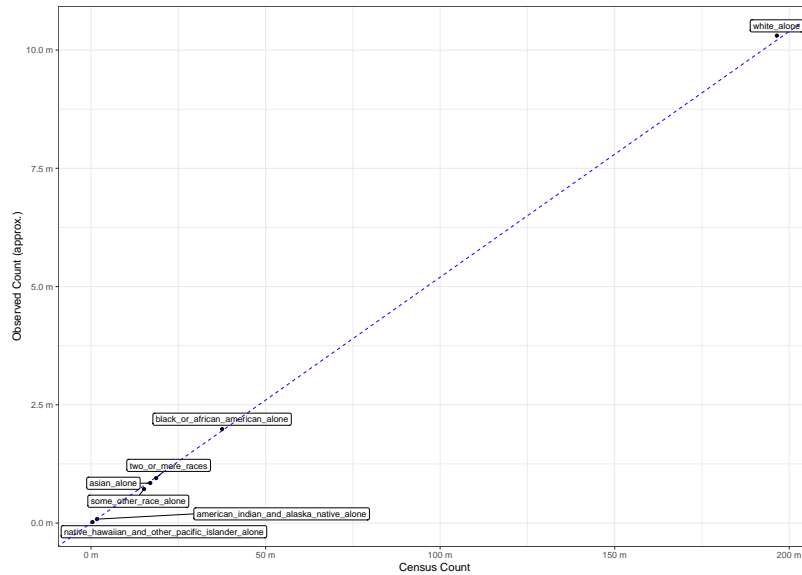
The plot shows how the age distribution of the SafeGraph users (y-axis) relates to the age distribution recorded by the census (x-axis). Both axes count the number of individuals in million (m). For representativeness the counts should line up along the diagonal line in blue.

Figure 9: Representativeness of SafeGraph data in terms of education



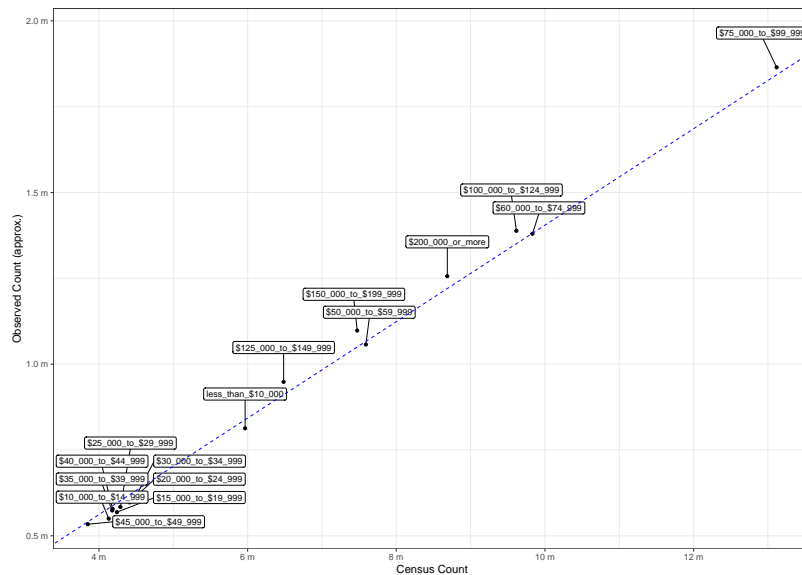
The plot shows how the education distribution of the SafeGraph users (y-axis) relates to the education distribution recorded by the census (x-axis). Both axes count the number of individuals in million (m). For representativeness the counts should line up along the diagonal line in blue.

Figure 10: Representativeness of SafeGraph data in terms of race



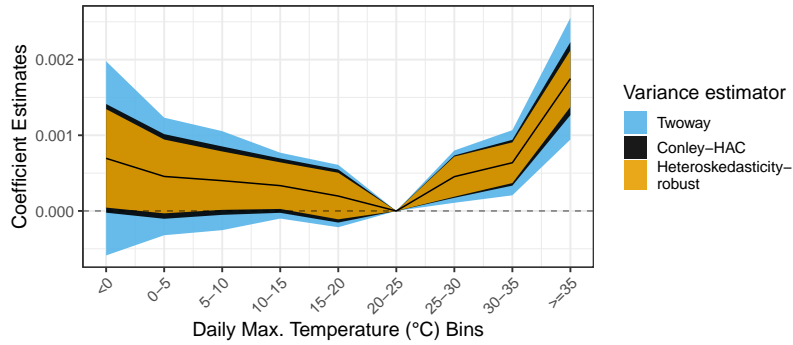
The plot shows how the race distribution of the SafeGraph users (y-axis) relates to the race distribution recorded by the census (x-axis). Both axes count the number of individuals in million (m). For representativeness the counts should line up along the diagonal line in blue.

Figure 11: Representativeness of SafeGraph data in terms of income



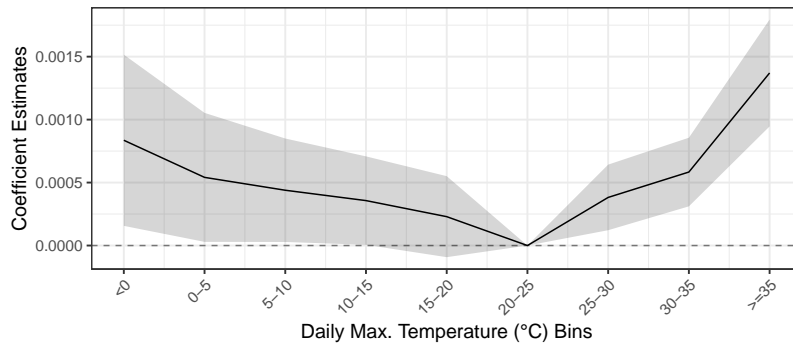
The plot shows how the income distribution of the SafeGraph users (y-axis) relates to the income distribution recorded by the census (x-axis). Both axes count the number of individuals in million (m). For representativeness the counts should line up along the diagonal line in blue.

Figure 12: Comparison to robust and twoway clustered standard errors



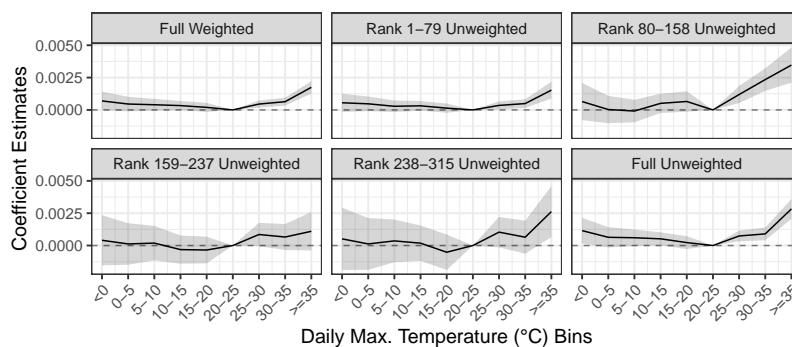
The figure shows the coefficients estimated for each of the daily maximum temperature bins excluding the 20°C to 25°C reference bin based on Eq. 8 and weighting by MSA population size. The colored areas depict asymptotic 95% confidence intervals based on heteroskedasticity-robust standard errors in orange, Conley-HAC standard errors in black, and twoway clustered standard errors in blue.

Figure 13: Sample based on urban areas



The figure shows the coefficients estimated for each of the daily maximum temperature bins excluding the 20°C to 25°C reference bin based on Eq. 8. All variables are derived on the urban area (UA) level and observations are weighted by UA population size. The shaded areas depict asymptotic 95% confidence intervals based on Conley-HAC standard errors.

Figure 14: Estimations based on subsamples with different population size



Coefficients estimated for each of the daily maximum temperature bins excluding the 20°C to 25°C reference bin based on Eq. 8. We consider six subsamples based on MSA population size as indicated by the respective subheadings. The subheadings also indicate whether observations are weighted by MSA population size. The shaded areas depict asymptotic 95% confidence intervals based on Conley-HAC standard errors.

Appendix Tables

Table 1: Top ten cities with decreasing encounters

MSA	Present-2050 total change in encounters (in millions)	
	under SSP5/RCP8.5	under SSP1/RCP2.6
Dallas, TX	8.0	4.9
Houston, TX	6.9	4.8
Tampa, FL	4.7	3.5
Miami, FL	4.7	2.6
San Antonio, TX	3.7	2.5
Orlando, FL	3.5	2.7
Kansas City, MO-KS	2.8	1.9
St. Louis, MO-IL	2.7	1.5
Atlanta, GA	2.7	1.4
Chicago, IL-IN-WI	2.7	1.4

Projected decreases in the total number of encounters in millions per city in 2050 under climate scenarios SSP1/RCP2.6 and SSP5/RCP8.5.